Title: **Orbitofrontal cortex, dorsolateral prefrontal cortex, and hippocampus represent the magnitude of event saliency**

Abbreviated title: **Neural representation of event saliency magnitude**

Author names and affiliation, including postal codes

Anna Jafarpour [1,2,3], Sandon Griffin [1], Jack J. Lin [4], Robert T. Knight [1,2]

1. Helen Wills Neuroscience Institute, University of California, Berkeley, CA 94720, USA
2. Department of Psychology, University of California, Berkeley, CA 94720, USA
3. Department of Physiology and Biophysics, University of Washington, WA 98195, USA
4. Department of Neurology and Biomedical Engineering, University of California, Irvine, CA 92697, USA

Corresponding author with complete address, including an email address and postal code

Anna Jafarpour; Department of Physiology and Biophysics, University of Washington, 1705 NE Pacific St., HSB Box 357290, Seattle, WA 98195; annaja@uw.edu

Conflict of Interest: The authors declare no competing financial interests.

Acknowledgements: The authors are indebted to the patients for their participation. We thank Jie Zheng and members of the Knightlab for helping with data collection. This work was sponsored by NINDS R37 NS21135 to RTK and the UC Irvine School of Medicine Bridge Fund to JJL.

Abstract

People fluidly segment a flow of events to establish a cognitive map of the ongoing environment, a process referred to as event-segmentation. The hippocampus and the prefrontal cortex encode cognitive maps, in which events in temporal or spatial proximity are more similarly represented than distant events. Hippocampal and prefrontal activity is also increased with detection of a deviant event. It is unclear whether the increased activity during event-segmentation is a deviant-detection response or also represents saliency magnitude, and how these contribute to constructing cognitive maps. We studied the regional response to a naturalistic fellow of events with varying saliency magnitudes. Using intracranial electroencephalography from ten patients, we observed that high-frequency activity (HFA; 50-150 Hz) in the hippocampus, dorsolateral prefrontal cortex, and orbitofrontal cortex tracked event saliency magnitudes. We propose that event saliency magnitude determines the contextual update for generating the cognitive map of events so that a sequence of less salient events is embedded in the context of more salient events. This dynamic contextual update can be used to generate a hierarchical map of the environment reflecting event contextual closeness.

Main

"I was waiting at home for my friend. I make some tea, washed the cups, and poured hot water. Then I felt everything shaking. It was an earthquake. I put the cup down and waited to see if there was an aftershock. Just about then, my friend arrived." People segment a stream of events into events (i.e. episodes) to parse what is happening at the moment (Zwaan and Radvansky, 1998); a process called event-segmentation (Zacks and Swallow, 2007; Zacks et al., 2007). In this process, sequences of events are organized to create a hierarchical clustering of events. The clustering generates a cognitive map of events' temporal order (Kurby and Zacks, 2008; Zacks and Swallow, 2007; Zwaan and Radvansky, 1998), wherein a sequence of less salient episodes are embedded in more salient overriding episodes (Zacks et al., 2007). In this example, making some tea was embedded in a friend's visiting.

A cognitive map reflects how similar or close events are to each other. The hippocampus (HPC) and the orbitofrontal cortex (OFC) represent cognitive maps (O'Keefe and Nadel, 1978; Schuck et al., 2016; Tolman, 1948; Wikenheiser and Schoenbaum, 2016). The hippocampal spatial representations are similar for contexts with small changes, but with an aberration, the contextual representation shifts or remaps (Bostock et al., 1991; Markus et al., 1995; Wills et al., 2005). Detecting the magnitude of deviation is important for appropriating updating the context and constructing a representative cognitive map. The HPC, OFC, and dorsolateral prefrontal cortex (PFC) are also engaged in detecting salient events (Knight, 1996, 1984; Nobre et al., 1999; Zacks et al., 2007) and in anticipation (Hindy et al., 2016; Hsieh et al., 2014; Jafarpour et al., 2017; Miller and Cohen, 2001; Motzkin et al., 2014). An outstanding question is whether the neural activities in the prefrontal cortex and the HPC indicate deviant detection per se or do they additionally capture the magnitude of event saliency needed for updating the environment.

It is also unclear if the deviant detection for an anticipated change in event context is larger than that for novel events. Salient events can be either novel (in this example, the earthquake was novel because it was out of context) or anticipated (in the example, the friend's arrival was anticipated.) Disentangling anticipated surprise and novelty in experimental conditions is difficult (Zarcone et al., 2016). Previous studies used a discrete experimental design, comparing the neural activity at the time of perceiving deviant events (i.e. event-boundaries (Kurby and Zacks, 2011)) to the neural activity at the time of perceiving non-boundary events (Speer et al., 2007; Whitney et al., 2009; Zacks et al., 2001). However, after encountering the first few deviant events, participants anticipate perceiving more surprises; thus, the later deviant events are no longer novel. A naturalistic flow of events has numerous event-boundaries with a range of saliency providing an ideal experimental design to address these issue. We employed a movie with such properties. The movie had three main parts. The first and the last parts had an unforeseeable storyline, but event boundaries in the second part of the movie were anticipated. This design allowed us to study neural activity during deviant detection, incorporating the magnitude of deviance and the anticipation parameter.

We recorded local field potential using intracranial electroencephalography (iEEG) from ten patients with epilepsy, who had the electrodes implemented for clinical purposes. Participants passively watched the movie (Figure 1), which was a mute animation (https://youtu.be/Q_guH9vA0sk). The first part the movie showed pairs of animals being in love, but there was a lonely lion looking for love who was attracted to a female lion. The second part showed that the lonely lion competed with another lion over multiple vying for the female lion's attention. The last part showed that the lonely lion lost the competition and moved on. We predicted that events bracketed by lower neural represent the context of low salient events and would be embedded in event structures for highly salient events in the hierarchical structure (Figure 1). Accordingly, prefrontal and hippocampal activities would correlate with the magnitude of event saliency needed to construct such an embedding cognitive map, and this effect would be more organized and stronger when salient events were anticipated in the middle part of the movie than the first or last parts of the movie.

We focused our analysis to local activity captured as the power in the high-frequency activity (HFA, 50 – 150 Hz) that serves as a metric for local neural activation (Belitski et al., 2008; Ray et al., 2008a) ; Jacobs and Kahana, 2009; Lachaux et al., 2012; Rich and Wallis, 2017). Power in HFA can also reflect increased temporal coherence of neural firing (Quyen et al., 2010; Ray et al., 2008a), or increased number of engaged neurons, perhaps because the stimuli is more demanding.

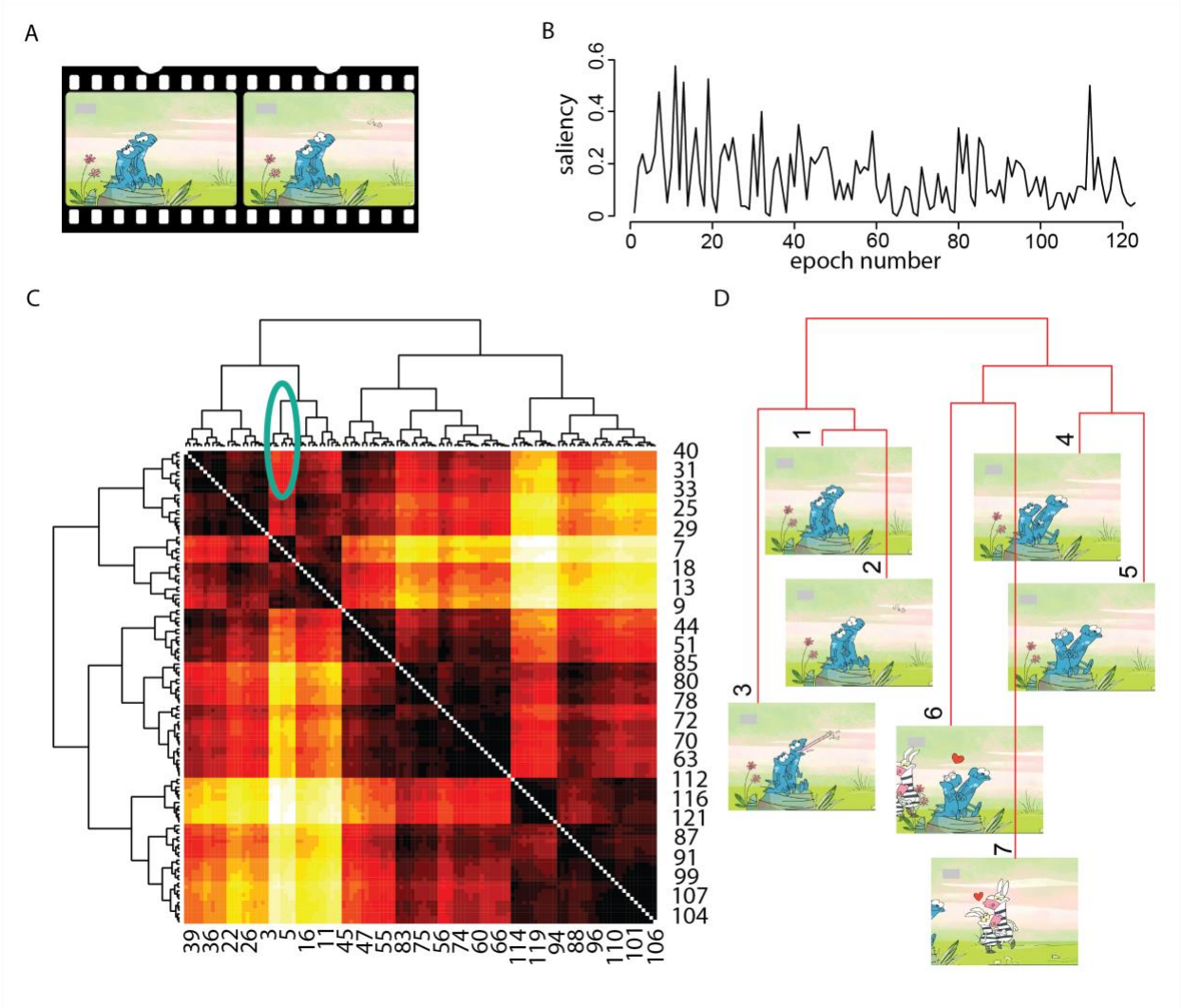

Figure 1. Hierarchical structure of the movie

(A) A 3-minute movie was chunked into 123 epochs of 1.5 seconds. (B) The epochs had a range of event saliency. (C) Event saliency was used to construct the hierarchical clustering to define event-segmentation. The heat map shows the sum of saliency of the events that occurred in between each pair of events. The row and column order have been re-ordered based on the hierarchical clustering results. All the epochs are displayed and the epoch number of every other five epoch is listed (the first row is epoch 40 and the last column is epoch 106). Temporally adjacent events are next to each other. The right and left branches of the hierarchy does not imply any order and can be flipped. This graph demonstrates that the movie consisted of three main parts with the similar lengths. (D) Zoomed in view of the first 10.5 seconds of the movie (marked branches in C). The graph shows the frames of the start of the story in the hierarchical cluster.

Results

We identified the magnitude of salient events in the movie by studying a separate group of adults (n = 80). This group indicated when during the movie a new episode started (i.e. perceiving an event-boundary). The metric of event saliency magnitude was the number of identified event-boundaries in a short time-window of the movie (about 20 frames or 1.5 seconds; Figure 1B; total movie time was 3 minutes). Epochs of 1.5 seconds resulted in saliency magnitude of 0 to 0.6 (1 would be the maximum saliency magnitude when every participant agrees that during the same 1.5 seconds an event boundary occurred). A distance matrix was constructed from the sum of saliency of events that occurred between pairs of events and was used for binary hierarchical event clustering (see the methods; Figure 1).

We tested the hypothesis that the magnitude of event saliency was tracked in the targeted regions. Ranked (Spearman) correlation and non-parametric permutation tests for statistical results were applied. The interchangeable non-overlapping HFA in 1.5 sec epochs allowed using non-parametric permutation testing. Cluster corrected p-values are reported.

We observed that the HFA correlated with the magnitude of event saliency that was captured by the behavior of the independent rating group. The neural effect was clustered in dorsolateral PFC (BA 6, 8, 9, and 10; in 6 out of 7 patients). The effect was also detected in the HPC (BA 54; in 3 out of 3 patients) and medial OFC (BA 11; in 4 out of 4 patients; Figures 3). See Tables 2 for statistical results.

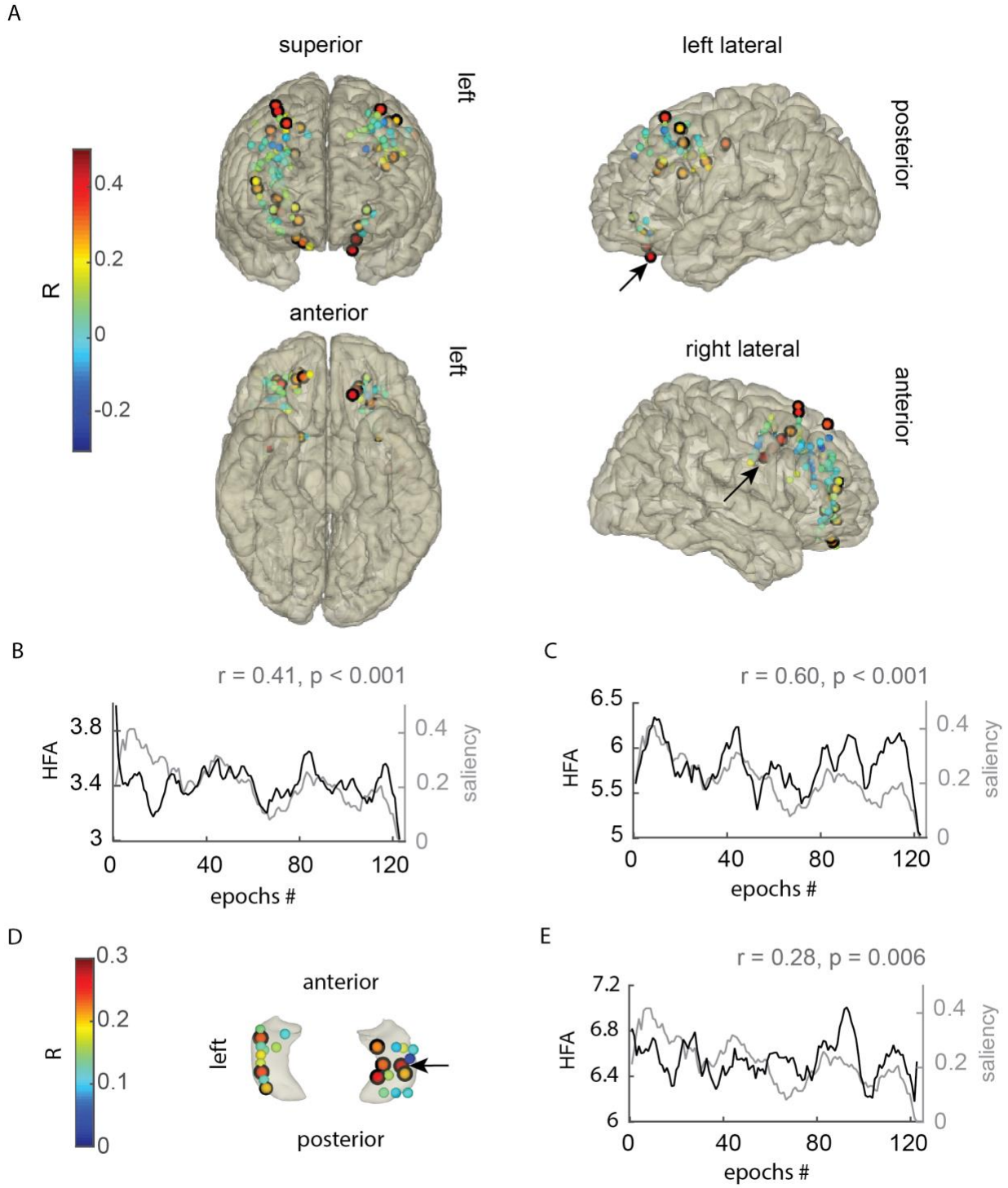
A
superior
left
left lateral
posterior
R
0.4
0.2
0
-0.2
anterior
left
right lateral
anterior
B
r = 0.41, p < 0.001
HFA
3.8
3.4
3
0.4
0.2
0
saliency
0
40
80
120
epochs #
C
r = 0.60, p < 0.001
HFA
6.5
6
5.5
5
0.4
0.2
0
saliency
0
40
80
120
epochs #
D
R
0.3
0.2
0.1
0
anterior
left
posterior
E
r = 0.28, p = 0.006
HFA
7.2
6.8
6.4
6
0.4
0.2
0
saliency
0
40
80
120
epochs #

Figure 2. Magnitude of event saliency was tracked in dorsolateral PFC, medial OFC, and the HPC

(A) HFA in the dorsolateral PFC and medial OFC increased with increasing magnitude of event saliency. The contacts are color-coded by the Spearman correlation coefficient (R) between the HFA and the magnitude of event saliency across 1.5-second epochs, which ranged between -0.3 and 0.7. (B) The saliency of each epoch (in gray) and HFA across epochs in a left medial OFC contact for example (in black). For demonstration, HFA and saliency were smoothed by a 10-episode window. (C) the same as (B) but for in a right dorsolateral PFC contact. (D) HFA in the hippocampus also correlated with event saliency magnitude. (E) An example of HFA in the hippocampus across epochs and the epochs saliency magnitude (same as B and C). (A and D) The black outlines highlight the contacts that showed the effect (cluster correct p-value < 0.05). The thickness of black outline reflects the effect significance (See table 1 for p-values). And the arrows show which contact corresponds to the plot B, C, and E. (B, C, and E) All examples were from patient #6.

Table 1. Statistical results

The table lists the participant names, Spearman correlation coefficient r, cluster corrected p-value, and the MNI coordinates of the contact in millimeters and RAS: positive x = right, positive y = anterior, and positive z = superior. The contacts are sorted according to their localization into the HPC, OFC, or PFC, as observed in the MRI scan in native space.

Participant number	r	p	x	y	z
HPC					
1	0.257	0.021	-32.42	-17.61	-13.84
1	0.251	0.025	-32.85	-33.69	-5.65
5	0.273	0.006	22.62	-15.30	-18.68
5	0.217	0.044	35.49	-16.88	-14.58
5	0.230	0.031	22.39	-29.53	-9.728
6	0.246	0.011	25.13	-21.11	-13.12
6	0.283	0.002	33.78	-20.60	-11.82
OFC					
1	0.305	0.003	16.26	45.28	-22.26
1	0.271	0.005	20.11	44.06	-19.80
4	0.263	0.004	19.01	47.55	-8.65

	6	0.410	< 0.001	-14.80	34.05	-27.56
	6	0.456	< 0.001	-17.17	36.55	-20.63
	6	0.241	0.009	-18.54	39.42	-12.64
PFC						
	2	0.280	0.012	-45.65	-0.92	32.36
	4	0.350	0.003	26.82	41.96	51.74
	4	0.391	0.001	32.04	23.65	59.05
	4	0.352	0.003	33.25	23.40	63.07
	4	0.349	0.003	-32.37	25.08	60.27
	6	0.369	0.001	30.23	40.62	-2.91
	6	0.279	0.013	32.44	43.05	4.80
	6	0.602	< 0.001	37.97	1.86	30.73
	6	0.539	< 0.001	37.01	7.27	36.46
	6	0.409	< 0.001	36.53	13.01	41.85
	6	0.308	0.005	36.32	18.54	47.24
	6	0.268	0.022	-40.57	13.40	44.16
	6	0.302	0.005	-26.79	29.02	26.59
	6	0.291	0.005	-40.40	27.15	30.77
	6	0.397	< 0.001	-37.94	-12.53	42.31
	6	0.465	< 0.001	-45.67	-12.97	43.13
	6	0.336	0.001	-52.64	-13.45	43.82
	8	0.248	0.004	44.84	47.47	10.89
	9	0.231	0.013	18.2	7.735	49.02
	9	0.247	0.008	-37.13	14.50	52.60
	9	0.215	0.025	-42.09	15.50	53.60
	10	0.245	0.024	21.50	39.55	32.72
	10	0.258	0.013	-35.98	13.74	25.19

A planned post-hoc analysis was done on the contacts that showed the effect (table 1) to study the specificity of the effect to the movie storyline. We calculated the Spearman correlation coefficient between the HFA and event saliency magnitude in three main parts of the movie (Figure 1, the first 3 branches/clusters). The first and the last part of the movie were similarly unpredictable. In contrast, the flow of events in the middle of the movie was unpredictable but anticipated. The results showed an effect of brain region on the correlation coefficient during the middle of the movie ($F(2,29) = 10.3$, $P <$

0.001). The correlation coefficient was higher for the OFC (r = 0.55, SD = 0.16; P = 0.002) and PFC (r = 0.45, SD = 0.13; P <0.001) than the HPC (mean r = 0.24, SD = 0.08). Furthermore, the correlation coefficient in OFC (first part mean Spearman r = 0.2, SD = 0.09; second part r = 0.55, SD = 0.16) and PFC (first part r = 0.32, SD = 0.2; second part r = 0.45, SD = 0.13; Figure 3) was higher during the middle part of the movie than the beginning or ending of the movie (OFC first vs middle: P = 0.031, OFC middle vs last: P = 0.031, PFC first vs middle: P = 0.031, PFC middle vs last: P <0.001), although there was no effect of brain region on the sum of HFA across the movie parts (F(2,29) = 0.84, P = 0.44 for the middle part of the movie), and the saliency of events was higher during the first part of the movie than second or last part of the movie. The saliency magnitude during the whole first part of the movie was in average 0.19 (SD = 0.15), the second part was 0.13 (SD = 0.10), and the last part of the movie was 0.12 (SD = 0.9).

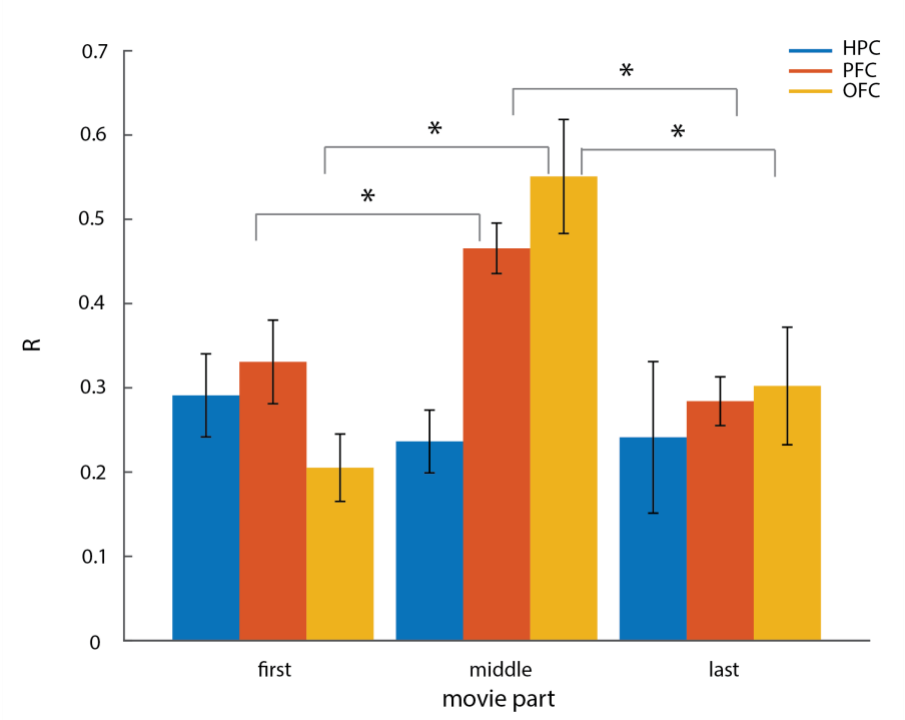

Figure 3. The HFA-saliency magnitude correlation coefficients (R) were strongest during the middle part of the movie, when the event boundaries were anticipated, in the OFC and dorsolateral PFC (* P < 0.05).

Discussion

Event segmentation theory suggests that a sequence of events is constructed into a cognitive map representing the contextual structure of the sequence (Kurby and Zacks, 2008; Zacks and

Swallow, 2007; Zwaan and Radvansky, 1998). The cognitive map has clusters of events, with less salient events embedded in more salient events (see also Collin et al., 2017). To construct a cognitive map, the magnitude of event saliency needs to be detected to track contextual relevance (Figure 1). Accordingly, less salient events would cluster within similar temporal contexts; whereas higher saliency events would shift the temporal context relative to their saliency magnitude. Lower saliency clusters would be embedded in a pyramid structured by higher saliency events. Here we report distributed neural regions that detect the magnitude of deviance in a flow of events to construct a cognitive map.

We used event segmentations of a large control population (behavior group) watching the same movie to infer the structure of neural cognitive map in another group of participants with intracranial electrodes (iEEG group). The behavior group's event-segmentation provided the saliency magnitude for the entire movie (Figure 1). The iEEG group passively watched a movie and did not know about the segmentation task, allowing us to study spontaneous neural processing of event parsing. We observed that event saliency HFA magnitude, linked to nearby SUA activity (Belitski et al., 2008; Jacobs and Kahana, 2009; Lachaux et al., 2012; Ray et al., 2008; Rich and Wallis, 2017) increased in hippocampus (HPC) and dorsolateral and orbital PFC (Figure 2).

We observed that the HFA in the dorsolateral PFC in the iEEG group tracked event saliency magnitude. Dorsolateral PFC is critical for guiding attention (Corbetta and Shulman, 2002; Hopfinger et al., 2000; Kastner et al., 1999; Paus, 1996) and increased HFA while perceiving salient events may be due to increased attention toward the salient events (Ray et al., 2008b; Zacks et al., 2001). Dorsolateral PFC is also engaged in cognitive control and conflict monitoring (MacDonald et al., 2000; Miller and Cohen, 2001). For example, PFC detects new associations of categories and exemplars (Dolan and Fletcher, 1997). We suggest that the correlation between HFA and event saliency magnitude reflects the demand for updating the 'event model' because a deviant detection signal requires an update of the current context (Reynolds et al., 2007; Zacks et al., 2007).

We also observed a similar saliency effect in the medial OFC (BA 11 but not in the dorsolateral OFC; Figure 4) with medial OFC activity stronger for high versus low less salient events. This effect is akin to the representation of saliency in the non-human primates' OFC, captured by HFA (Rich and Wallis, 2016, 2017). In humans, breaching expectations increases activity in the OFC (Duarte et al., 2009; Mikutta et al., 2015; Nobre et al., 1999). Here, we propose that OFC may represent the saliency magnitude for constructing the structure of event context. Thus, with greater deviance the context is shifted more, allowing one to construct a hierarchical structure of contexts. The idea of OFC representing a context, such as a hierarchical structure, has also been proposed for task structures and concepts (Schuck et al., 2016; Wilson et al., 2014).

The magnitude of event saliency also correlated with HFA in the HPC (Figure 2, and Table 1). HPC activity is linked to the representation of event structure (Ekstrom et al., 2003; Mack et al., 2017; Quiroga, 2012; Quiroga et al., 2005). HPC remaps with greater changes in the environment, providing a hierarchical cognitive map in rodents (Shapiro et al., 1997) and perhaps in humans (Chen et al., 2015). A recent studie showed that the HPC representations also reflect the magnitude of topological saliency of an environment (Javadi et al., 2017) and the magnitude of deviance from expectation (Figure 2) (Chen et al., 2015). Indeed, deviant detection effects HPC activities (Axmacher et al., 2010; Chen et al., 2013, 2015; Knight, 1996; Kumaran and Maguire, 2007; Lisman and Otmakhova, 2001; Strange et al., 1999; Wittmann et al., 2007). Here, we propose that the magnitude of deviance may be essential for accurately updating the context so that a small deviance induces only a small change in the ongoing temporal context. This idea agrees with the notion that close events share more similar HPC representations than far events (Collin et al., 2015; Ezzyat and Davachi, 2014).

Oftentimes changing expectations are anticipated and sometimes deviant events are novel (the event is out of the scope of contextual constraints). Anticipation based on the gist of previous experience shapes event structures (Allan T. Purcell, 1986; Reynolds et al., 2007). The magnitude of anticipation increases the PFC activity in both dorsolateral PFC and the medial OFC; Bechara et al., 1996; Critchley et al., 2001). A closer look at our data showed that the

effects in the OFC and dorsolateral PFC were stronger when event boundaries were anticipated (Figure 3). This implies that the PFC does not purely detect the magnitude of deviance; it anticipates the deviance. The anticipation may tune the firing rate of the PFC neurons resulting in the observed increased correlation between HFA and saliency magnitude.

An important question concerns the dynamics of interaction in the neural network for saliency detection and event segmentation. For example, disturbing the input from the HPC to OFC impairs representing task structures in rodents (Wikenheiser et al., 2017). It is not clear if the hippocampal deviant detection is essential for constructing the OFC signal in humans or if other brain regions such as mid-brain structures contribute to detecting the magnitude of deviance (Dürschmid et al., 2016; Wittmann et al., 2007). For instance, HPC responses to the deviant events are associated with activity in the substantia nigra and ventral tegmental area (Wittmann et al., 2007). It is also suggested that the HPC provides a novelty signal to the Nucleus Accumbens (Dürschmid et al., 2016). Moreover, while HPC activity is linked to anticipation (Hindy et al., 2016; Hsieh et al., 2014; Jafarpour et al., 2017), it is unclear if the prediction is made by the HPC or other brain regions such as the PFC. A caveat of this iEEG study is that the patients did not have coverage from multiple regions to definitively study the dynamics of the network.

A change in the flow of events requires an update in the temporal context and the cognitive map. Medial OFC and HPC represent cognitive maps (O'Keefe and Nadel, 1978; Tolman, 1948; Wikenheiser and Schoenbaum, 2016; Wilson et al., 2014) and activity in both brain regions increases when detecting deviant events (Axmacher et al., 2010; Bunzeck et al., 2010; Chen et al., 2013; Knight, 1996; Kumaran and Maguire, 2007; Long et al., 2016; Strange et al., 2005). Here we show that HPC, dorsolateral PFC, and orbital PFC constitute three core regions of the network need to update our cognitive maps according to the magnitude of event salience - less salient events clustered within a similar temporal context and embedded under more salient events to construct a cognitive map of the world.

Methods

Approval

The study protocol was approved by the Office for the Protection of Human Subjects of the University of California, Berkeley, the University of California, Irvine, and Stanford University. All participants provided written informed consent before participating.

Participants

Intracranial EEG: Ten epileptic patients who had stereo-tactically implanted depth electrodes to localize the seizure onset zone for subsequent surgical resection participated in this study, (Table 2). The electrodes were placed at the University of California, Irvine Medical Centre with 5-mm inter-electrode spacing. All participants had normal (or corrected) vision. No seizures occurred during task administration. Neural activity was inspected by two independent neurologists. Only contacts in the non-epileptic brain areas were included for analysis. Electrode coverage varied, in the medial temporal lobe and the prefrontal cortex depending on their clinical requirements (Figure 4). Electrodes were localized in the patient's native space, then transferred to MNI space for visualizing the group coverage. Note that two out of five participants had dorsolateral OFC coverage and three out of five had medial OFC contacts.

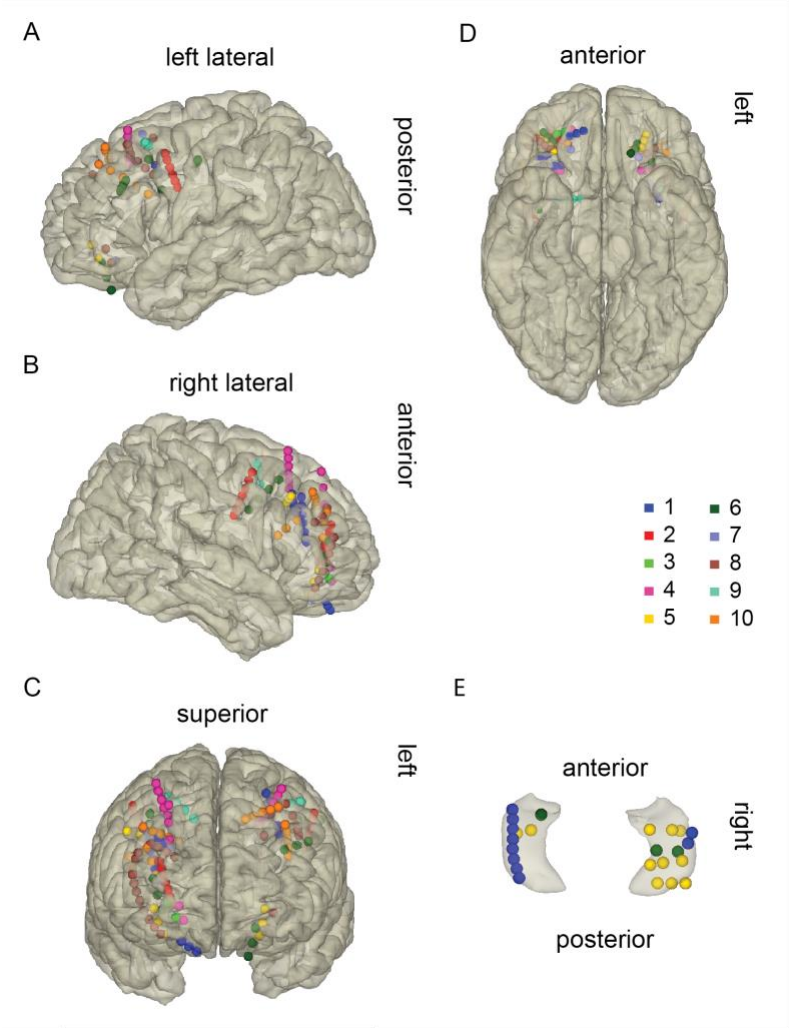

Figure 4. The contact coverage of the participants is color-coded by patients' number. (A-D) shows the PFC and OFC coverage from (A) the right sagittal, (B) the left sagittal, (C) the coronal, and (D) the inferior view. (E) shows the hippocampal coverage in a 3D glass hippocampus from the superior anterior view.

Table 2. Patient electrode coverage

This table contains the age, gender, dominant hand, and the electrode coverage of each iEEG participants. The X denotes if the patient had coverage in OFC, HPC, or lateral PFC.

Patient	Age	Gender	Dominant hand	OFC coverage	HPC coverage	Lateral PFC coverage

1	50	Male	Right	X	X	
2	46	Male	Right			X
3	26	Male	Right	X		
4	31	Male	Left	X		X
5	40	Female	Left		X	
6	58	Female	Right	X	X	X
7	34	Male	Right			X
8	22	Female	Right	X		X
9	33	Male	Right			X
10	23	Male	Right			X

Behavioral experiment: A control group of 80 healthy adults participated in a movie segmentation test (53 female, mean age = 27.93, SD = 13.91, age range = 18 to 68 years old). 31 participants were 18 to 21 years old, 29 participants were 21 to 30 years old, and 20 participants were older than 30 years old.

Experimental design

Participants watched a mute short animation (~3minutes long). The movie had an overarching cliché love triangle story. The movie was a short version of the animation designed by Ali Derakhshi, named "wildlife" or "Hayat-e Vahsh", the episode on lions (https://youtu.be/Q_guH9vA0sk). The movie was selected so that the visual angle was kept similar (Fig. 1A). The iEEG group passively watched the muted movie.

The behavioral control group watched the movie and concurrently segmented the movies into episodes. We instructed them to press a key "whenever something new happened." We clarified that "we want to segment this movie into episodes". After the segmentation task, they performed a target detection task. A target was displayed at random intervals. Participants were instructed to press a key as soon as they perceived the target. The aim of this part of the experiment was to measure participants' response time for normalization purposes across subjects.

Behavioral analysis

Key press timing was recorded during segmentation and target detection tasks. Participants' response time was measured as the difference between the target onsets and the responses. The averaged response-time per participant was subtracted from the timing of keypress for movie segmentation to infer the timing of event boundaries. We excluded consecutive keypresses for segmentation if the interval was less than 100ms (double key registration). The number of segmented events was accumulated across participants at 1.5 sec time bins. The number of events in 1.5 sec time bins reflected the saliency of events. An event was more salient if more people reported it as an event boundary, and an event was less salient if a fewer people marked them as an event boundary (Figure 1). The hierarchical event-segmentation is constructed from the distance between two events, that was measured by adding the saliency magnitude of all the events between the two events. Events were in distant branches if highly salient events were in between them; otherwise, events were in the same branch.

iEEG data collection and preprocessing

Intracranial EEG data were acquired using the Nihon Kohden recording system, analog-filtered above 0.01 Hz and digitally sampled at 5 KHz or 10 KHz. A photodiode recorded the luminance of a corner of the screen to track the timing of movie presentation. A neurologist selected the contacts that showed epileptic activities and epochs with seizure spread. Only contacts in non-pathological regions were included in the analysis.

All EEG analyses were run in R (R Development Core Team, 2014), Matlab 2015a, and fieldtrip toolbox (Oostenveld et al., 2010) offline. Artifact rejection was performed on the raw signal and any contaminated epileptic activities were removed. We applied a 2 Hz stopband Butterworth notch filter at 60 Hz line power noise and harmonics and then down-sampled the data to 1 KHz using resample() Matlab function via fieldtrip (Oostenveld et al., 2010). The function applies an antialiasing FIR lowpass filter and compensates for the delay introduced by the filter. All contacts were re-referenced to a neighboring contact (i.e. bipolar reference). The continuous signal was then cropped in 1.5 sec long epochs with no overlaps. The epochs were bandpass

filtered for high-frequency activity (HFA; 50 to 150 Hz) using padding and a Hamming window. The Hilbert transformation was applied to the filtered data for extracting the power.

Statistical Analysis for correlation between the HFA and event saliency

We used Spearman correlation to examine the relationship between the probability of perceiving a new event and the power. Interchangeable non-overlapping 1.5 sec epochs were used for non-parametric statistical permutation testing. The null distribution was generated by surrogating trial labels in 1000 iterations. In each iteration, the maximum correlation between power and the probability (of perceiving a new event) was taken across all contacts in the region of interest for each participant to construct the null distribution. The proportion of correlation coefficients that was more than that observed correlation coefficient in the null-distribution yielded the non-parametric corrected p-value for the observed correlation. The p-value < 0.05 was considered significant.

How much was the effect was dependent on the movie's storyline?

We tested the correlation between the magnitude of event saliency and HFA in each brain region across three main parts of the movie (Figure 1, first 3 branches/clusters). The first and the last parts had surprising stories. The first part showed that many pairs of animals were in love and a lonely lion was seeking love. The last part shows that the lion lost in a competition and travels to find love elsewhere. The second part of the movie showed that the lion vied over multiple games and points were counted at the end of each game. This section had a routine. Although the timing of the end of a game was unpredictable, there was an anticipation for ongoing competitions (https://youtu.be/Q_guH9vA0sk). The correlation coefficients within each region were compared to others using two-sided Wilcoxon rank sum test for the middle part of the story.

Electrode localization and visualization

Electrode locations were reconstructed and visualized in MATLAB using the Fieldtrip toolbox (Stolk et al.). To maximize the accuracy of the reconstructions, electrodes were manually selected on the post-implantation CT, which was co-registered to the pre-implantation MRI using SPM (Ashburner and Friston, 1997). The locations of the electrodes were identified by a neurologist. Electrode positions were then obtained in MNI space by normalizing each subject's pre-implantation MRI to the MNI152 template brain using SPM (Ashburner and Friston, 1999).

Representations of the cerebral cortex were generated using FreeSurfer (Dale et al., 1999). Representations of the hippocampus were generated from the Desikan-Killiany atlas (Desikan et al., 2006) using Fieldtrip (Stolk et al.). The Brodmann areas were inferred from Bioimage Suite package (http://bioimagesuite.yale.edu/).

The hierarchical clusters for Figure 1 were constructed from the magnitude of the event saliency. The distance between two epochs was the sum of saliency of events in between those two. The distance between two events was large if many highly salient events occurred in between them, and the distance between them was small if not highly salient events occurred. The hierarchical clustering was performed in R (R Development Core Team, 2014).

Reference

Allan T. Purcell (1986). Environmental Perception and Affect: A Schema Discrepancy Model. Environment and Behavior *18*, 3–30.

Ashburner, J., and Friston, K.J. (1997). Multimodal image coregistration and partitioning — a unified framework. Neuroimage *6*, 209–217.

Ashburner, J., and Friston, K.J. (1999). Nonlinear Spatial Normalization using Basis Functions. Human Brain Mapping *7*, 254–266.

Axmacher, N., Cohen, M.X., Fell, J., Haupt, S., Dümpelmann, M., Elger, C.E., Schlaepfer, T.E., Lenartz, D., Sturm, V., and Ranganath, C. (2010). Intracranial EEG Correlates of Expectancy and Memory Formation in the Human Hippocampus and Nucleus Accumbens. Neuron *65*, 541–549.

Bechara, A., Tranel, D., Damasio, H., and Damasio, A.R. (1996). Failure to Respond Autonomically to Anticipated Future Outcomes Following Damage to Prefrontal Cortex. Cereb Cortex *6*, 215–225.

Belitski, A., Gretton, A., Magri, C., Murayama, Y., Montemurro, M.A., Logothetis, N.K., and Panzeri, S. (2008). Low-Frequency Local Field Potentials and Spikes in Primary Visual Cortex Convey Independent Visual Information. J. Neurosci. *28*, 5696–5709.

Bostock, E., Muller, R., and Kubie, J. (1991). Experience-dependent modifications of hippocampal place cell firing. Hippocampus *1*, 193–206.

Bunzeck, N., Dayan, P., Dolan, R.J., and Duzel, E. (2010). A common mechanism for adaptive scaling of reward and novelty. Hum. Brain Mapp. *31*, 1380–1394.

Chen, J., Dastjerdi, M., Foster, B.L., LaRocque, K.F., Rauschecker, A.M., Parvizi, J., and Wagner, A.D. (2013). Human hippocampal increases in low-frequency power during associative prediction violations. Neuropsychologia *51*, 2344–2351.

Chen, J., Cook, P.A., and Wagner, A.D. (2015). Prediction strength modulates responses in human area CA1 to sequence violations. Journal of Neurophysiology *114*, 1227–1238.

Collin, S.H., Milivojevic, B., and Doeller, C.F. (2017). Hippocampal hierarchical networks for space, time, and memory. Current Opinion in Behavioral Sciences *17*, 71–76.

Collin, S.H.P., Milivojevic, B., and Doeller, C.F. (2015). Memory hierarchies map onto the hippocampal long axis in humans. Nat Neurosci *18*, 1562–1564.

Corbetta, M., and Shulman, G.L. (2002). CONTROL OF GOAL-DIRECTED AND STIMULUS-DRIVEN ATTENTION IN THE BRAIN. Nature Reviews Neuroscience *3*, 215–229.

Critchley, H.D., Mathias, C.J., and Dolan, R.J. (2001). Neural Activity in the Human Brain Relating to Uncertainty and Arousal during Anticipation. Neuron *29*, 537–545.

Dale, A.M., Fischl, B., and Sereno, M.I. (1999). Cortical Surface-Based Analysis. NeuroImage *9*, 179–194.

Desikan, R.S., Ségonne, F., Fischl, B., Quinn, B.T., Dickerson, B.C., Blacker, D., Buckner, R.L., Dale, A.M., Maguire, R.P., Hyman, B.T., et al. (2006). An automated labeling system for subdividing the human cerebral cortex on MRI scans into gyral based regions of interest. NeuroImage *31*, 968–980.

Dolan, R.J., and Fletcher, P.C. (1997). Dissociating prefrontal and hippocampal function in episodic memory encoding. Nature *388*, 582.

Duarte, A., Henson, R.N., Knight, R.T., Emery, T., and Graham, K.S. (2009). Orbito-frontal Cortex is Necessary for Temporal Context Memory. Journal of Cognitive Neuroscience *22*, 1819–1831.

Dürschmid, S., Zaehle, T., Hinrichs, H., Heinze, H.-J., Voges, J., Garrido, M.I., Dolan, R.J., and Knight, R.T. (2016). Sensory Deviancy Detection Measured Directly Within the Human Nucleus Accumbens. Cereb Cortex *26*, 1168–1175.

Ekstrom, A., Kahana, M., Caplan, J., Fields, T., Isham, E., Newman, E., and Fried, I. (2003). Cellular networks underlying human spatial navigation. Nature *425*, 184–188.

Ezzyat, Y., and Davachi, L. (2014). Similarity breeds proximity: Pattern similarity within and across contexts is related to later mnemonic judgments of temporal proximity. Neuron *81*, 1179–1189.

Hindy, N.C., Ng, F.Y., and Turk-Browne, N.B. (2016). Linking pattern completion in the hippocampus to predictive coding in visual cortex. Nat Neurosci *19*, 665–667.

Hopfinger, J.B., Buonocore, M.H., and Mangun, G.R. (2000). The neural mechanisms of top-down attentional control. Nature Neuroscience; New York *3*, 284–291.

Hsieh, L.-T., Gruber, M.J., Jenkins, L.J., and Ranganath, C. (2014). Hippocampal Activity Patterns Carry Information about Objects in Temporal Context. Neuron *81*, 1165–1178.

Jacobs, J., and Kahana, M.J. (2009). Neural Representations of Individual Stimuli in Humans Revealed by Gamma-Band Electrocorticographic Activity. J. Neurosci. *29*, 10203–10214.

Jafarpour, A., Piai, V., Lin, J.J., and Knight, R.T. (2017). Human hippocampal pre-activation predicts behavior. Scientific Reports *7*, 5959.

Javadi, A.-H., Emo, B., Howard, L.R., Zisch, F.E., Yu, Y., Knight, R., Silva, J.P., and Spiers, H.J. (2017). Hippocampal and prefrontal processing of network topology to simulate the future. Nature Communications *8*, 14652.

Kastner, S., Pinsk, M.A., De Weerd, P., Desimone, R., and Ungerleider, L.G. (1999). Increased Activity in Human Visual Cortex during Directed Attention in the Absence of Visual Stimulation. Neuron *22*, 751–761.

Knight, R. (1996). Contribution of human hippocampal region to novelty detection. Nature *383*, 256–259.

Knight, R.T. (1984). Decreased response to novel stimuli after prefrontal lesions in man. Electroencephalography and Clinical Neurophysiology/Evoked Potentials Section *59*, 9–20.

Kumaran, D., and Maguire, E.A. (2007). Match mismatch processes underlie human hippocampal responses to associative novelty. J. Neurosci. *27*, 8517–8524.

Kurby, C.A., and Zacks, J.M. (2008). Segmentation in the perception and memory of events. Trends Cogn. Sci. (Regul. Ed.) *12*, 72–79.

Kurby, C.A., and Zacks, J.M. (2011). Age differences in the perception of hierarchical structure in events. Mem Cogn *39*, 75–91.

Lachaux, J.-P., Axmacher, N., Mormann, F., Halgren, E., and Crone, N.E. (2012). High-frequency neural activity and human cognition: Past, present and possible future of intracranial EEG research. Progress in Neurobiology *98*, 279–301.

Lisman, J.E., and Otmakhova, N.A. (2001). Storage, recall, and novelty detection of sequences by the hippocampus: Elaborating on the SOCRATIC model to account for normal and aberrant effects of dopamine. Hippocampus *11*, 551–568.

Long, N.M., Lee, H., and Kuhl, B.A. (2016). Hippocampal mismatch signals are modulated by the strength of neural predictions and their simi- larity to outcomes. J. Neurosci. 1850–16.

MacDonald, A.W., Cohen, J.D., Stenger, V.A., and Carter, C.S. (2000). Dissociating the Role of the Dorsolateral Prefrontal and Anterior Cingulate Cortex in Cognitive Control. Science *288*, 1835–1838.

Mack, M.L., Love, B.C., and Preston, A.R. (2017). Building concepts one episode at a time: The hippocampus and concept formation. Neuroscience Letters.

Markus, E.J., Qin, Y.L., Leonard, B., Skaggs, W.E., McNaughton, B.L., and Barnes, C.A. (1995). Interactions between location and task affect the spatial and directional firing of hippocampal neurons. J. Neurosci. *15*, 7079–7094.

Mikutta, C.A., Dürschmid, S., Bean, N., Lehne, M., Lubell, J., Altorfer, A., Parvizi, J., Strik, W., Knight, R.T., and Koelsch, S. (2015). Amygdala and orbitofrontal engagement in breach and resolution of expectancy: A case study. Psychomusicology: Music, Mind, and Brain *25*, 357–365.

Miller, E.K., and Cohen, J.D. (2001). An Integrative Theory of Prefrontal Cortex Function. Annual Review of Neuroscience *24*, 167–202.

Motzkin, J.C., Philippi, C.L., Wolf, R.C., Baskaya, M.K., and Koenigs, M. (2014). Ventromedial Prefrontal Cortex Lesions Alter Neural and Physiological Correlates of Anticipation. J. Neurosci. *34*, 10430–10437.

Nobre, A.C., Coull, J.T., Frith, C.D., and Mesulam, M.M. (1999). Orbitofrontal cortex is activated during breaches of expectation in tasks of visual attention. Nat Neurosci *2*, 11–12.

O'Keefe, J., and Nadel, L. (1978). The Hippocampus as a Cognitive Map (Oxford University Press).

Oostenveld, R., Fries, P., Maris, E., Schoffelen, J.-M., Oostenveld, R., Fries, P., Maris, E., and Schoffelen, J.-M. (2010). FieldTrip: Open Source Software for Advanced Analysis of MEG, EEG, and Invasive Electrophysiological Data, FieldTrip: Open Source Software for Advanced Analysis of MEG, EEG, and Invasive Electrophysiological Data. Computational Intelligence and Neuroscience, Computational Intelligence and Neuroscience *2011*, *2011*, e156869.

Paus, T. (1996). Location and function of the human frontal eye-field: A selective review. Neuropsychologia *34*, 475–483.

Quiroga, R.Q. (2012). Concept cells: the building blocks of declarative memory functions. Nat Rev Neurosci *13*, 587–597.

Quiroga, R.Q., Reddy, L., Kreiman, G., Koch, C., and Fried, I. (2005). Invariant visual representation by single neurons in the human brain. Nature *435*, 1102–1107.

R Development Core Team (2014). R: A Language and Environment for Statistical Computing.

Ray, S., Niebur, E., Hsiao, S.S., Sinai, A., and Crone, N.E. (2008). High-frequency gamma activity (80–150Hz) is increased in human cortex during selective attention. Clinical Neurophysiology *119*, 116–133.

Reynolds, J.R., Zacks, J.M., and Braver, T.S. (2007). A Computational Model of Event Segmentation From Perceptual Prediction. Cognitive Science *31*, 613–643.

Rich, E.L., and Wallis, J.D. (2016). What stays the same in orbitofrontal cortex. Nat Neurosci *19*, 768–770.

Rich, E.L., and Wallis, J.D. (2017). Spatiotemporal dynamics of information encoding revealed in orbitofrontal high-gamma. Nature Communications *8*, 1139.

Schuck, N.W., Cai, M.B., Wilson, R.C., and Niv, Y. (2016). Human Orbitofrontal Cortex Represents a Cognitive Map of State Space. Neuron *91*, 1402–1412.

Shapiro, M.L., Tanila, H., and Eichenbaum, H. (1997). Cues that hippocampal place cells encode: dynamic and hierarchical representation of local and distal stimuli. Hippocampus *7*, 624–642.

Speer, N.K., Zacks, J.M., and Reynolds, J.R. (2007). Human Brain Activity Time-Locked to Narrative Event Boundaries. Psychological Science *18*, 449–455.

Stolk, A., Griffin, S., van der Meij, R., Dewar, C., Saez, I., Lin, J.., Piantoni, G., Schoffelen, J.-M., Knight, R.T., and Oostenveld, R. An integrated platform for human intracranial data analysis.

Strange, B., Duggins, A., Penny, W., Dolan, R., and Friston, K. (2005). Information theory, novelty and hippocampal responses: unpredicted or unpredictable ? Neural Networks *18*, 225–230.

Strange, B.A., Fletcher, P.C., Henson, R.N., Friston, K.J., and Dolan, R.J. (1999). Segregating the functions of human hippocampus. Proc Natl Acad Sci U S A *96*, 4034–4039.

Tolman, E.C. (1948). Cognitive maps in rats and men. Psychological Review *55*, 189–208.

Whitney, C., Huber, W., Klann, J., Weis, S., Krach, S., and Kircher, T. (2009). Neural correlates of narrative shifts during auditory story comprehension. NeuroImage *47*, 360–366.

Wikenheiser, A.M., and Schoenbaum, G. (2016). Over the river, through the woods: cognitive maps in the hippocampus and orbitofrontal cortex. Nat Rev Neurosci *17*, 513–523.

Wikenheiser, A.M., Marrero-Garcia, Y., and Schoenbaum, G. (2017). Suppression of Ventral Hippocampal Output Impairs Integrated Orbitofrontal Encoding of Task Structure. Neuron *95*, 1197–1207.e3.

Wills, T.J., Lever, C., Cacucci, F., Burgess, N., and O'Keefe, J. (2005). Attractor Dynamics in the Hippocampal Representation of the Local Environment. Science *308*, 873–876.

Wilson, R.C., Takahashi, Y.K., Schoenbaum, G., and Niv, Y. (2014). Orbitofrontal cortex as a cognitive map of task space. Neuron *81*, 267–279.

Wittmann, B.C., Bunzeck, N., Dolan, R.J., and Düzel, E. (2007). Anticipation of novelty recruits reward system and hippocampus while promoting recollection. NeuroImage *38*, 194–202.

Zacks, J.M., and Swallow, K.M. (2007). Event Segmentation. Current Directions in Psychological Science *16*, 80–84.

Zacks, J.M., Braver, T.S., Sheridan, M.A., Donaldson, D.I., Snyder, A.Z., Ollinger, J.M., Buckner, R.L., and Raichle, M.E. (2001). Human brain activity time-locked to perceptual event boundaries. Nat Neurosci *4*, 651–655.

Zacks, J.M., Speer, N.K., Swallow, K.M., Braver, T.S., and Reynolds, J.R. (2007). Event perception: a mind-brain perspective. Psychol Bull *133*, 273–293.

Zarcone, A., van Schijndel, M., Vogels, J., and Demberg, V. (2016). Salience and Attention in Surprisal-Based Accounts of Language Processing. Front. Psychol. *7*.

Zwaan, R.A., and Radvansky, G.A. (1998). Situation models in language comprehension and memory. Psychological Bulletin *123(2)*, 162–185.